Atomic Oxygen Effects on the Prefailure Damage Processes in Highly Filled Glass/Mica/Epoxy Composites

M. REGOLA,* E. BAER,† and A. HILTNER

Department of Macromolecular Science, Case Western Reserve University, Cleveland, Ohio 44106

SYNOPSIS

In the present study, the effect of atomic oxygen (AO) exposure, as a simulation of low earth orbit, on the flexural properties and prefailure damage mechanisms of a series of short glass fiber/mica/epoxy composites under three-point bending were elucidated using acoustic emission (AE) techniques. The incorporation of mica in the composites was shown to increase the resistance to AO as measured by the weight loss, ashing rate, and reaction efficiency. Furthermore, as the mica content increased, the resistance increased such that the all-mica composite had over one order of magnitude lower ashing rate and reaction efficiency than did the all-glass-fiber composite. This increased resistance was caused by the mica particles preferentially orienting parallel to the surface of the composites, creating an inorganic barrier to attack. The AO-induced erosion was found to have an insignificant effect on both the flexural properties and prefailure damage mechanisms because the erosion was confined to the epoxy surface only and did not affect the bulk.

INTRODUCTION

The space environment is composed of atomic oxygen (AO), ultraviolet (UV) radiation, high-energy electron and proton radiation, solar flare protons, and micrometeoroids and space debris. There are two predominant orbits that spacecraft operate in geosynchronous orbit (GEO) and low earth orbit (LEO). Communication and surveillance satellites operate in GEO, which is at 22,300 nmi. The primary concerns in GEO are UV, vacuum, thermal cycling, and ionizing radiation.[1]

LEO is where surveillance satellites, earth-sensing satellites, the space shuttle, and space station Freedom operate.[1] This orbit ranges from about 125–350 nmi and exposes materials to vacuum, UV radiation, electron bombardment, micrometeoroid impact, thermal cycling, and atomic oxygen. The durability of materials to this environment has been of great concern ever since the initial space shuttle flights detected substantial surface erosion of the polyimide film thermal control blankets.[2] It was found early on that atomic oxygen was responsible for this degradation and posed a serious threat to materials.[3-5]

Atomic oxygen is the predominant species in LEO and is formed by the dissociation of O_2 by UV (100–200 nm) radiation.[3,6] At orbital altitudes, the neutral atmosphere is primarily 80% AO and 20% N_2. The AO density exponentially decreases with increasing altitude and varies with the season, time of day, solar activity, and position (latitude and longitude).[3,6] Although the actual density is low, the motion of spacecraft through this residual atmosphere at velocities on the order of 7.5–8.0 km/s results in a high AO flux (approximately 10^{14}–10^{15} atoms/s cm^2) at high energies (about 4.5–5.0 eV).[3] Energies of this magnitude cause mass loss to materials such as polyimides, graphite–epoxy, carbon, and even some metals. During STS-5, -8, and -41G, surface recessions as high as 0.5 μm/orbit occurred for some materials.[6]

Because of the reactivity of AO with polymeric materials, the sensitivity to AO must be assessed before a material can be used for spacecraft applications. This can be accomplished in two ways: exposure to LEO, usually aboard the space shuttle, or

* Present address: Lord Corporation, 2000 West Grandview Blvd, Erie, PA 16514.

† To whom correspondence should be addressed.

Journal of Applied Polymer Science, Vol. 42, 2631–2642 (1991)
 CCC 0021-8995/91/102631-12$04.00

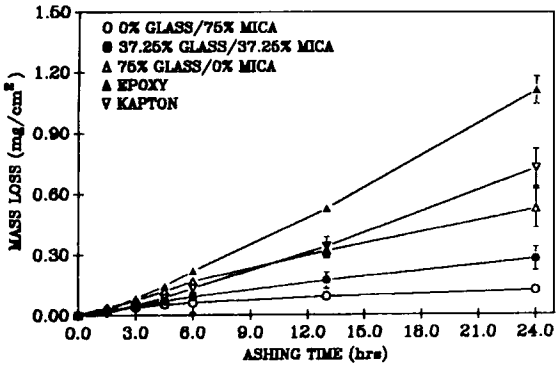

Figure 1. Short-term mass loss vs. ashing time for experimental data sets 1 and 2.

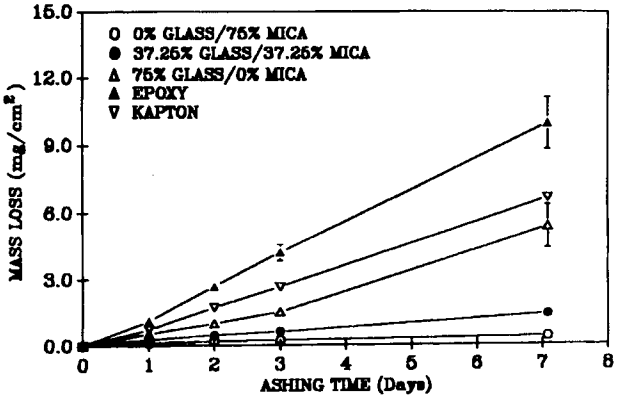

Figure 2. Long-term mass loss vs. ashing time for experimental data sets 1 and 2.

ground-based simulation of LEO. One instrument used for ground-based simulation of AO is a Plasma Prep II. This unit is often referred to as an asher since it was designed to remove organic materials from glassware, etc., by rapid oxidation. Rutledge et al. used the plasma asher to evaluate a mica-filled paint for protection of graphite–epoxy composites.[7] It was found that the mica is resistant to AO and that materials with larger percentages of mica exhibited larger initial protection. However, eventually, all the materials degraded at nearly the same rate as did the unprotected graphite–epoxy. It was thought that the mica paint was undercut by the AO since the asher produces a flux in all directions, leaving mica flakes lying on the surface that can easily be removed. Furthermore, air pockets in the paint can become ionized in the radio-frequency (RF) discharge, used to generate the AO, causing the paint to degrade from within.

Fiberglass–epoxy composites were exposed to AO generated by a Plasma Prep II to determine the extent of degradation by Rutledge et al.[8] Oxidation of the epoxy surface, exposing individual glass fibers that are easily removed, was observed. Contrary to the previous statement that the oxidation stability of organic materials is dependent on the oxidative stability of the fillers, the fiberglass did not enhance the AO protection. The mechanism of degradation was believed to be the breaking of chemical bonds such as C—C that subsequently allowed the surface to be oxidized. The mass loss, however, was not large enough to significantly change the tensile modulus of the composite.

There have been a number of space-based experiments performed, primarily on STS-5 and STS-8. The University of Alabama flew an experiment on STS-8 to investigate the effect of AO on optical systems, metals, various forms of carbon, and other surfaces.[9–11] The reaction rate of AO with various surfaces and its dependence on temperature was also

Table I Comparison of the Ashing Rates of the Glass/Mica Ratio Composites and a Comparison of the Reaction Efficiencies of the Glass/Mica Ratio Composites to Some Materials Exposed to LEO

Material	Ashing Rate ($\times 10^6$ mg/cm^2 s)	R_e ($\times 10^{24}$ cm^3/atom)	Reference
Glass/mica/epoxy			
0/75/25	0.64	0.22	—
37.25/37.25/25	2.30	0.78	—
75/0/25	8.79	2.96	—
0/0/100	16.3[a]	5.47	—
Kapton	10.9	3.0	1
Epoxy	—	1.7	8
Graphite epoxy			
1034C	—	2.1	8
5208/T300	—	2.6	8

[a] Normalized to Kapton control.

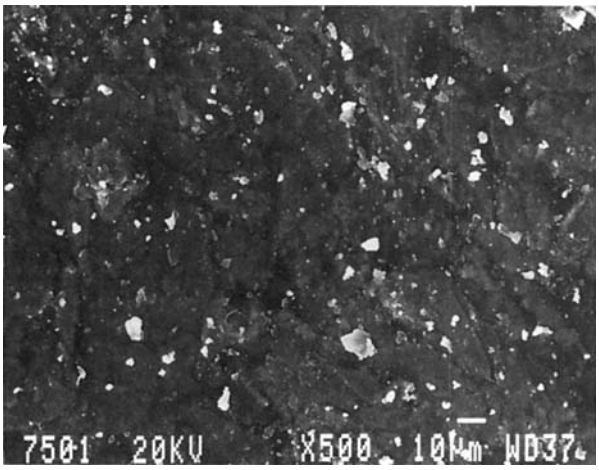

A. Unexposed to AO

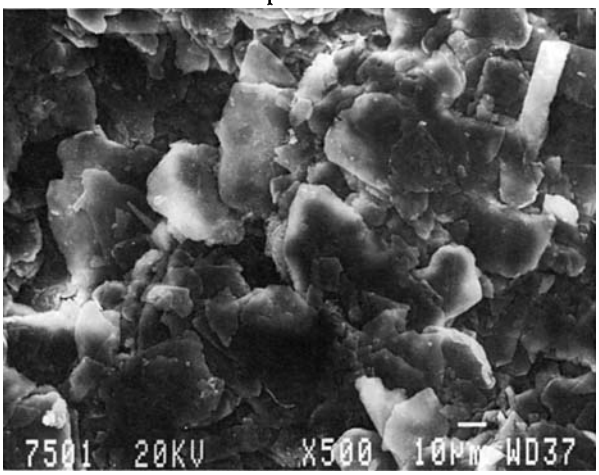

B. Exposed to AO for 7 days

Figure 3. Surface morphology of the 0% glass/75% mica composite unexposed (A) and exposed (B) to AO.

investigated. No induction time was observed before the onset of AO erosion. Furthermore, the reaction probabilities were found to depend on temperature. This indicates that synergistic effects can be important in the degradation of organic materials. Also, most carbonaceous surfaces exposed were heavily etched, with diamond being the least affected, while the metals were stable from a macroscopic standpoint except for osmium and silver. Other experiments on this flight as well as on STS-5 and STS-41G have shown that graphite and Kevlar fibers erode in AO with little residual strength and stiffness, that surface recession (or thickness loss) is proportional to fluence, and that the reaction rates for filled organic materials are dependent on the oxidative stability of the fillers.[12-14]

Obviously, ground-based testing has inherent advantages, such as cost. However, ground-based testing equipment such as the plasma asher cannot simulate the LEO environment accurately, so there is a fundamental question of quantifiability of the results obtained. Kiefer and Orwoll studied the oxidation products from several polymer systems obtained from exposure to a Plasma Prep II plasma generator and found fully oxidized products (i.e., H_2O, CO_2, NO_2, SO_2).[15] It was concluded that the asher is a suitable screening device for qualitative estimates of resistance of organic materials to AO. Rutledge et al. also studied this limitation and concluded that even though there is mainly nitrogen in the plasma the reacting species appears to be AO.[8]

It is the purpose of this paper to investigate the AO resistance of the glass/mica/epoxy composites in a qualitative manner, as well as determine the effect of exposure on the flexural properties and failure processes by utilizing a plasma asher to sim-

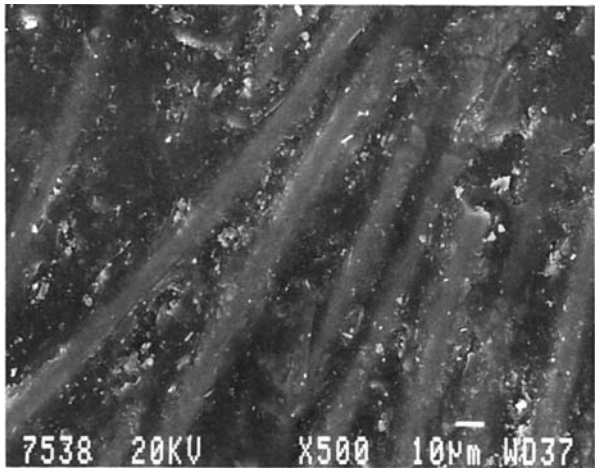

A. Unexposed to AO

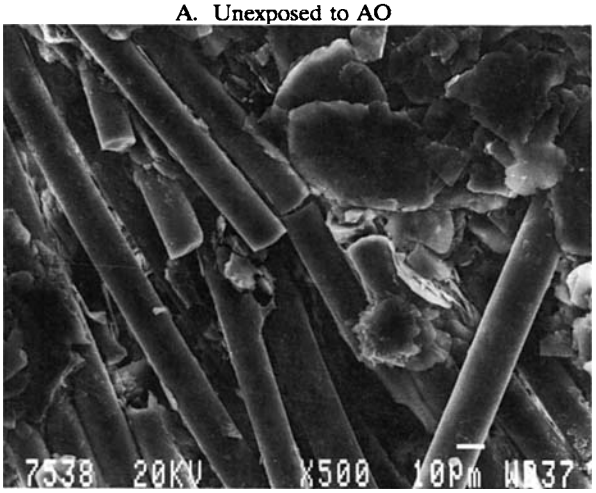

B. Exposed to AO for 7 days

Figure 4. Surface morphology of the 37.25% glass/37.25% mica composite unexposed (A) and exposed (B) to AO.

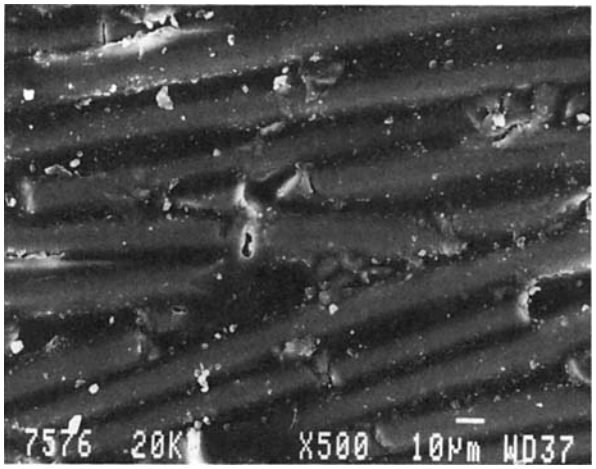

A. Unexposed to AO

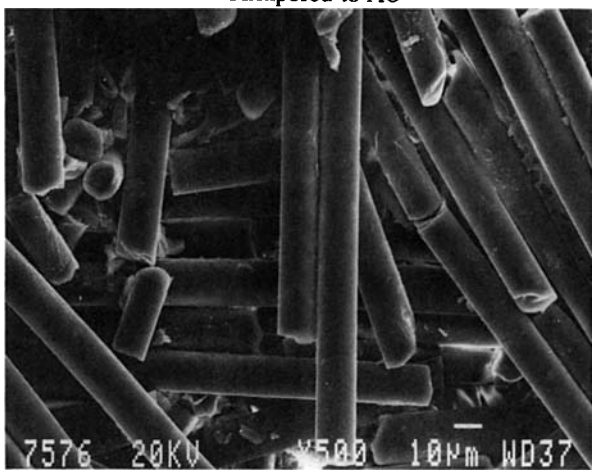

B. Exposed to AO for 7 days

Figure 5. Surface morphology of the 75% glass/0% mica composite unexposed (A) and exposed (B) to AO.

ulate the LEO environment. The effect of exposure on the surface morphology is also investigated.

EXPERIMENTAL

Analysis

Atomic Oxygen

Atomic oxygen exposure was conducted using an SPI Plasma Prep II RF plasma asher. This unit applies a radio-frequency field of 13.56 MHz to ambient air under low vacuum (approximately 30 mtorr), creating reactive ions of oxygen, nitrogen, and their related compounds. Materials that degrade in LEO always degrade in ashers, but materials that degrade in ashers do not necessarily degrade in LEO. Also, the rates of degradation between the asher and spe-

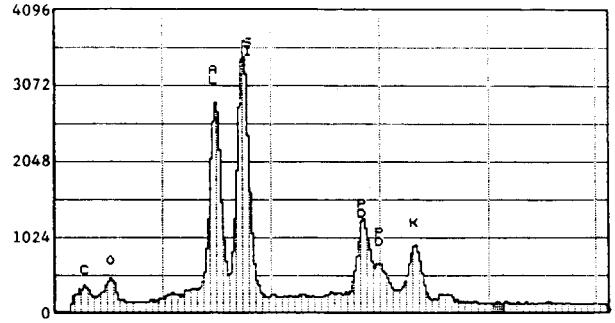

A. Unexposed to AO

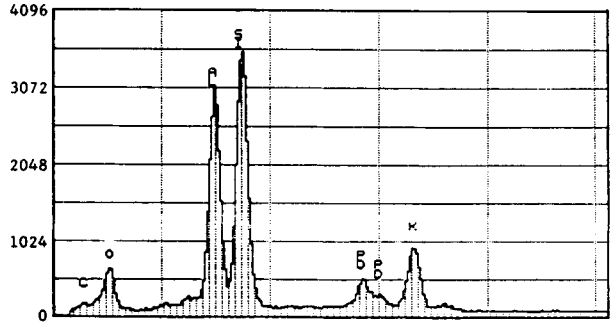

B. Exposed to AO for 7 days

Figure 6. Light element EDAX of the 0% glass/75% mica composite unexposed (A) and exposed (B) to AO.

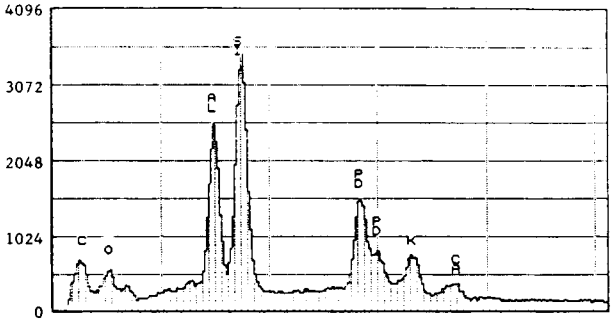

A. Unexposed to AO

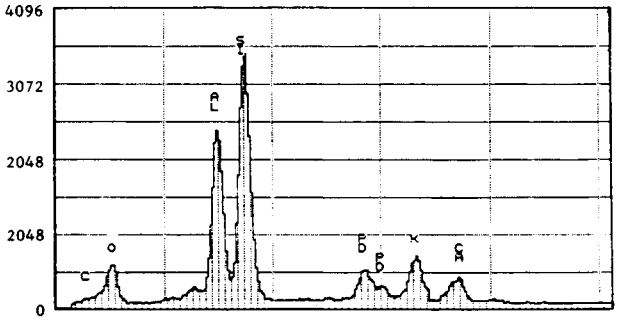

B. Exposed to AO for 7 days

Figure 7. Light element EDAX of the 37.25% glass/37.25% mica composite unexposed (A) and exposed (B) to AO.

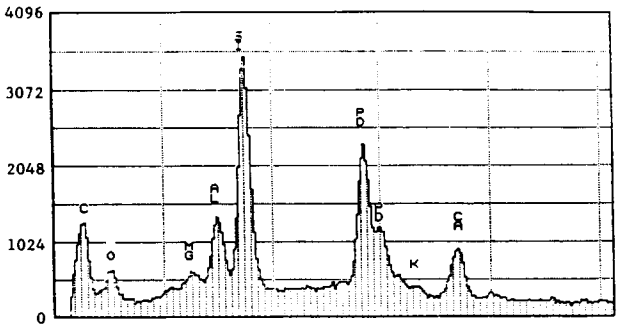

A. Unexposed to AO

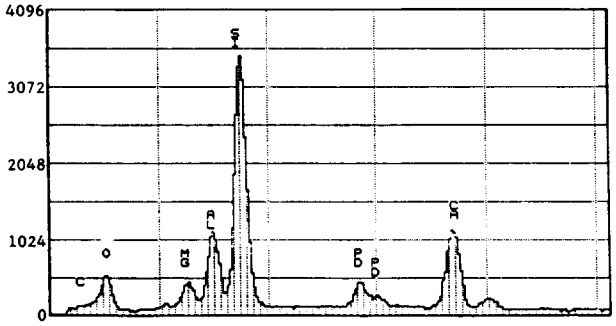

B. Exposed to AO for 7 days

Figure 8. Light element EDAX of the 75% glass/0% mica composite unexposed (A) and exposed (B) to AO.

cific altitudes in LEO differ depending on the material.[7] Thus, ashers give a qualitative measure of survivability but not a quantitative one.

The usual test protocol is to record the mass loss/unit area as a function of ashing time, reported in units of mg/cm^2. This is accomplished by periodically removing the sample from the asher and measuring its weight. The ashing rate, which is merely the slope from the initial point to the final point in the mass loss vs. ashing time curve, is also calculated and is reported in units of mg/cm^2 s. The reaction efficiency, R_e, also referred to as the erosion yield, is calculated as follows for materials exposed to LEO[12]:

$$R_e = \frac{\delta}{F}$$

where δ is the depth of material removed, given in cm, and F is the fluence of AO, given in atom/cm^2. This is reported in units of cm^3/atom and represents the volume of material lost per incident oxygen atom. This is a calculation performed on materials that are exposed to LEO and so has limited utility here because of the previously mentioned differences between the asher environment and LEO. However, given the mass loss of the composite obtained by the asher, the composite surface area, and the epoxy density (it is assumed that the matrix is the only constituent that erodes), a thickness loss can be calculated as follows:

$$\delta_C = \frac{\Delta m_C}{\rho_C A_C}$$

where the subscript C denotes composite, Δm is the change in mass, ρ is the density, and A is the surface area.

Similarly, the Kapton control surface recession is calculated as follows:

$$\delta_K = \left(\frac{\Delta m_K}{\rho_K A_K}\right)$$

The thickness loss of the composite is normalized with respect to the Kapton control by dividing δ_C

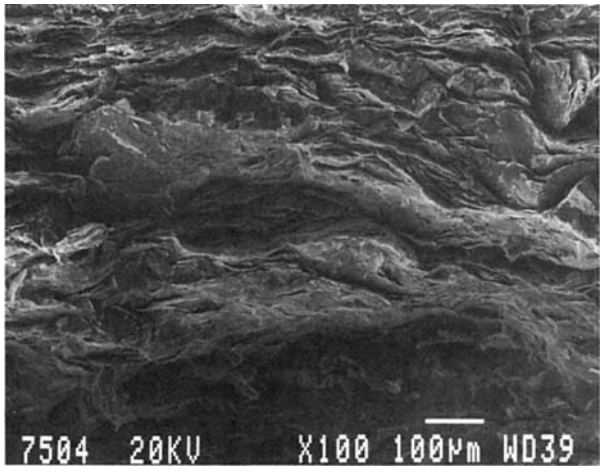

A.

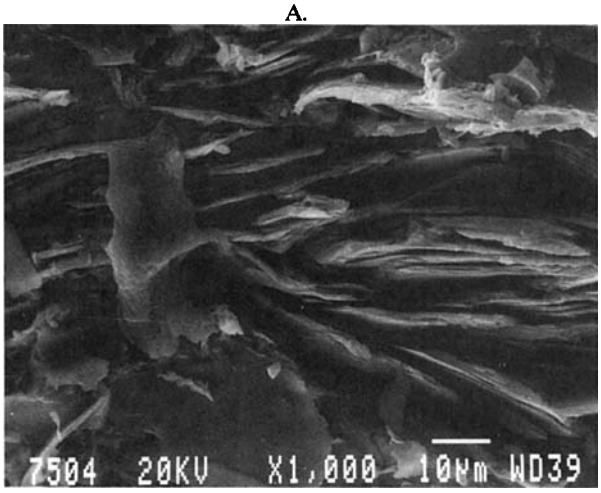

B.

Figure 9. Fracture surfaces of the exposed to AO 0% glass/75% mica composite at 100× (A) and 1000× (B) magnification.

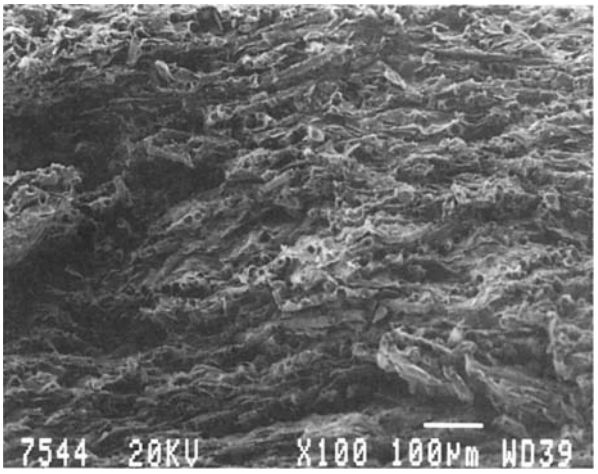

A.

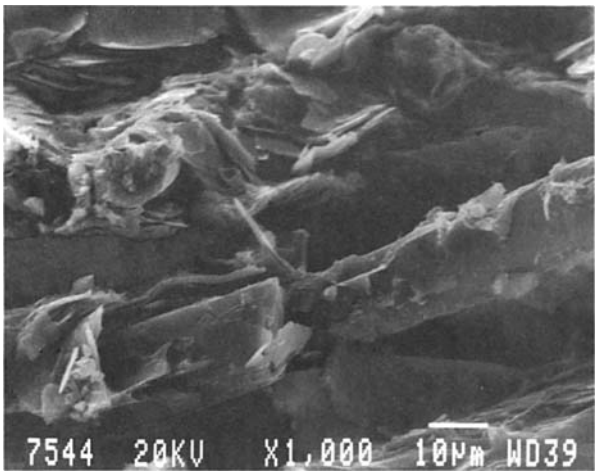

B.

Figure 10. Fracture surfaces of the exposed to AO 37.25% glass/37.25% mica composite at 100× (A) and 1000× (B) magnification.

by δ_K and then subsequently normalizing for LEO by multiplying this unitless value by the reaction efficiency of Kapton in LEO. This calculation yields a reaction efficiency as follows:

$$R_e = R_{e,K}\left(\frac{\delta_C}{\delta_K}\right)$$

where $R_{e,K} = 3 \times 10^{-24}$ cm^3/atom.

The 0% glass fiber/75% mica (0/75), 37.25/37.25, and 75/0 composites, as well Kapton, used as a control, were exposed to the asher for 170 h. To assure the mass loss was real and not caused by adsorbed water, the samples were dehydrated for at least 66 h prior to exposure. Also, the samples were kept in a desiccator while the weights were measured. The glass fiber/mica ratio samples and pure epoxy were tested in triplicate, and the averages and standard deviations of the mass loss/unit area values were calculated.

AE During Flexural Deformation

The composites exposed to AO were tested in three-point bending using an Instron Materials Tester 1123 according to ASTM-D790 with a crosshead speed of 0.1 mm/min with simultaneous AE monitoring. A span to depth ratio of 32 was chosen to minimize the contribution of shear in the measured properties.

Scanning Electron Microscopy

The surface morphology of the exposed composites was compared with the unexposed composites to give

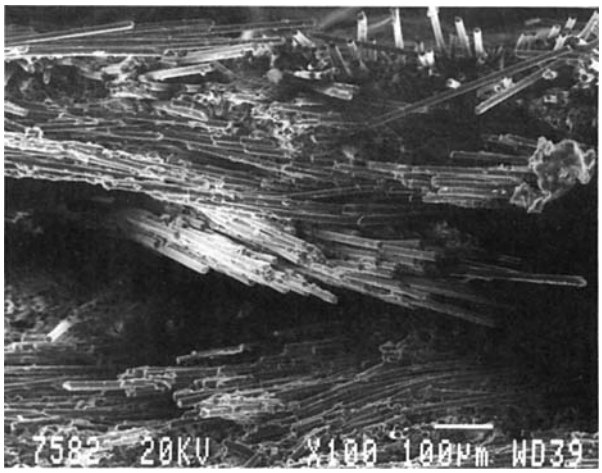

A.

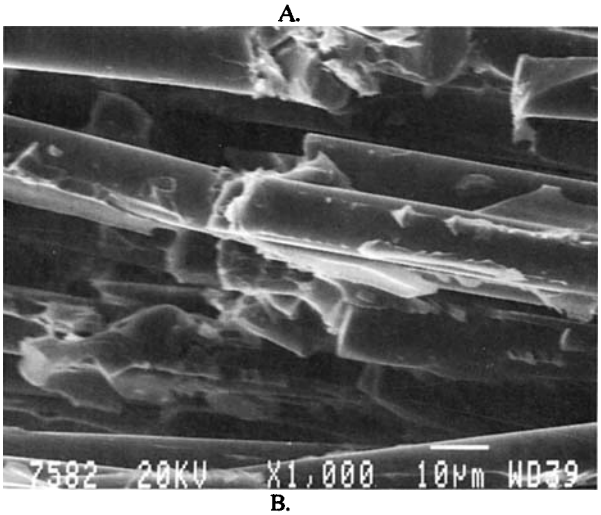

B.

Figure 11. Fracture surfaces of the exposed to AO 75% glass/0% mica composite at 100× (A) and 1000× (B) magnification.

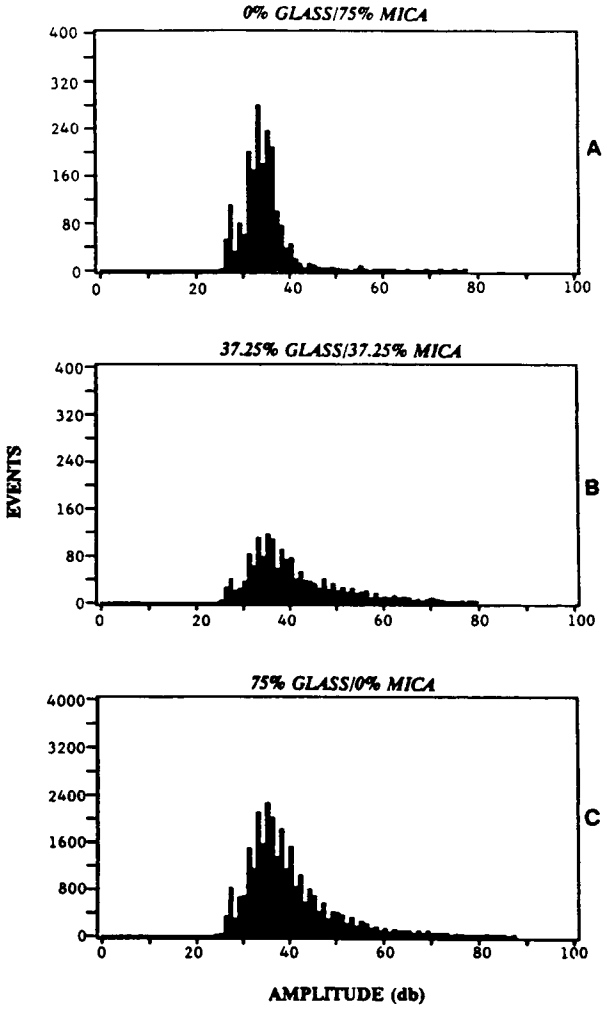

Figure 12. Compositional analysis of the exposed to AO composites showing their AE fingerprint.

insight into the AO degradation. The composites were coated with approximately 100 Å of palladium before observation at an acceleration voltage of 20 kV. Light element EDAX was performed on the exposed and unexposed composite surfaces at an acceleration voltage of 15 kV. This high voltage permitted penetration of the coating, giving a spectrum of the composite surface. Although a quantitative measurement of the elemental composition cannot be made with light element EDAX, comparison of peak heights can be made and will give some indication of which component is causing the mass loss.

Fracture surfaces were studied at predetermined locations to allow comparison of the exposed and unexposed to AO surfaces, allowing any differences in the damage processes to be assessed. The surfaces were coated with approximately 100 Å of palladium before observation.

RESULTS AND DISCUSSION

Atomic Oxygen Exposure

Mass Loss

The LEO AO environment was simulated using a plasma asher. Since weight changes on the order of 10^{-4} g were measured, dehydration of the materials was performed until a constant weight was obtained.

The mass loss, given in mg/cm^2, vs. ashing time for the first 24 h are shown in Figure 1. This figure shows the mass loss of the glass fiber/mica ratio composites, pure epoxy, and Kapton control. Since two different experimental sets were tested, the data are combined by normalizing to a constant Kapton mass loss. The initial behavior, up to 4.5 h, shows no significant differences between the composites. This is caused by the erosion of the epoxy surface layer, which would be expected to erode at the same rate independent of the underlying composition and is confirmed by the similar mass loss of the pure epoxy. After about 12 h, however, the differences become apparent as an increase in the mica content decreases the mass loss, which translates into an increased resistance to AO.

The long-term mass loss for the materials is shown in Figure 2, in which the same standardization of the data is done as before. The trend in the short-term exposure, that is, increasing mica content increases the AO resistance, continues for the duration of the exposure and becomes more pronounced as a function of time. Notice, however, a change in the slope of the all-glass-fiber composite from a slope intermediate between the 37.25/37.25 composite and epoxy before 3 days to a slope nearly equal to the epoxy after 3 days. This indicates that the glass fibers are offering only limited protection to the composite, which has been observed by others.[8] The incorporation of mica, however, gives much lower mass losses than the Kapton, epoxy, or the all-glass-fiber composite. The all-mica composite, for instance, has over one order of magnitude lower mass loss than does the Kapton. Increased resistance to AO by mica has been observed by Rutledge et al.[7] The proposed mechanism for the resistance is based on the plateletlike morphology of the mica particles. It was proposed that the mica would preferentially orient parallel to the surface, creating an inorganic barrier to AO attack. The mica was incorporated into a paint, however, and although an increase in the all-mica content gave increased resistance to AO, the paint medium still eroded and eventually all the materials eroded at the same rate as the uncoated

Table II Effect of AO Exposure on the Flexural Properties of the Glass Fiber/Mica Composites

Effect of Ashing on Initial Slope			
Formulation	Unashed ($\times 10^2$ lb/in.)[a]	Ashed ($\times 10^2$ lb/in.)	Ashed (Scraped) ($\times 10^2$ lb/in.)[b]
0% glass/75% mica	2.49	2.29	2.40
37.25% glass/37.25% mica	2.78	2.52	2.62
75% glass/0% mica	2.37	2.19	2.06
Effect of Ashing on Maximum Load			
Formulation	Unashed (lb)[a]	Ashed (lb)	Ashed (Scraped (lb)[b]
0% glass/75% mica	9.76	9.93	9.54
37.25% glass/37.25% mica	22.2	17.4	21.3
75% glass/0% mica	21.4	18.1	19.5
Effect of Ashing on Maximum Deflection			
Formulation	Unashed Deflection (in.)[a]	Ashed (in.)	Ashed (Scraped) (in.)[b]
0% glass/75% mica	0.44	0.46	0.43
37.25% glass/37.25% mica	0.94	0.87	0.92
75% glass/0% mica	0.93	0.95	0.89

Deviations are ±10%.
[a] Calculated from a previous dataset and normalized for thickness differences.
[b] Normalized for thickness change due to ashing.

material. Although the erosion does not stop in the composites of this study, it remains low throughout the test, indicating that incorporation of mica into the composite itself has advantages over using it merely in a coating.

Ashing Rates

The ashing rates, calculated from the initial and final points on the mass loss vs. ashing time curve, are shown in Table I. This, of course, reflects the characteristics of the mass loss behavior as the all-mica composite exhibits over one order of magnitude lower ashing rate than do the all-glass-fiber composite, epoxy, and Kapton control. The all-glass-fiber composite has a lower rate due to its initial behavior. The Kapton, used as a control, is seen to exhibit poor resistance to the asher environment. Kapton also erodes significantly in LEO and so can act as a base line for ordering the composites resistance to AO in that materials that perform worse than Kapton can be assumed to perform worse than do the composites in this study.

Reaction Efficiencies

As outlined in the Experimental section, a reaction efficiency can be calculated with the data obtained by the asher. The calculated reaction efficiencies are shown in Table I along with values for an epoxy and graphite epoxy that were exposed to LEO. The pure epoxy exposed to the asher would be expected to have approximately the same reaction efficiency as does the epoxy exposed to LEO if the environments are similar. Considering the experimental errors involved in the ashing experiments, the pure epoxy reaction efficiency is surprising close to the LEO epoxy reaction efficiency. The differences are due to the differences between the asher and LEO environments as outlined in the Introduction and supports the conclusion that the asher gives qualitative information only. Because the asher cannot make life-on-orbit predictions, it is desirable to expose these materials to the LEO environment. This will be done on STS-42, scheduled for launch April 4, 1991. Nonetheless, the reaction efficiencies confirm the mass loss and ashing rate conclusion that as the

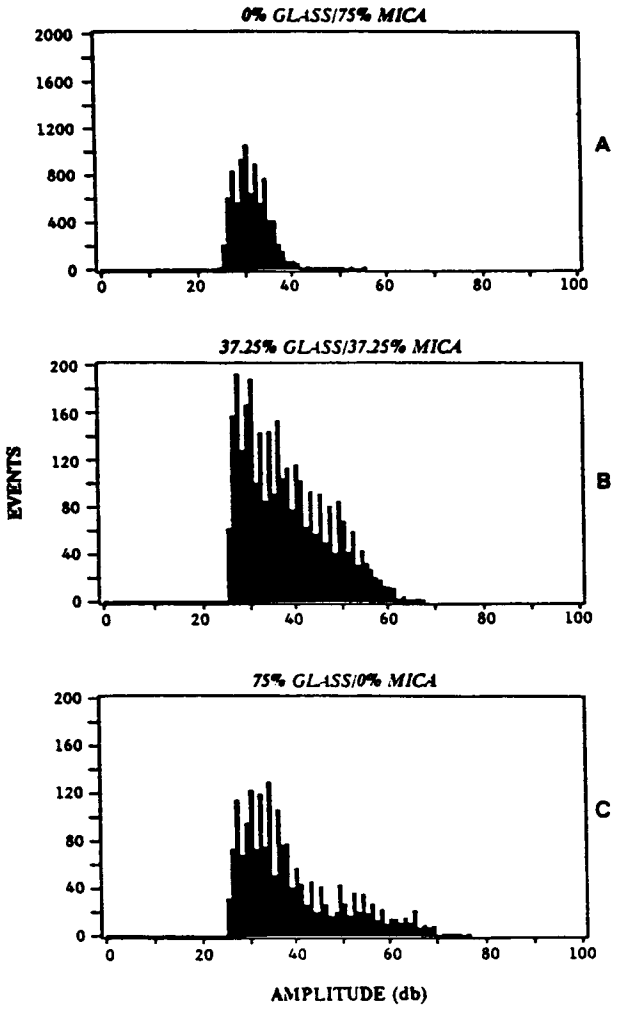

Figure 13. Compositional analysis of the unexposed composites showing their AE fingerprint.

mica content increases the resistance to AO increases.

Scanning Electron Microscopy

Surface Morphology of Composites

The surface morphology of the unashed and ashed all-mica composite is shown in Figure 3. Comparison of the two surfaces reveals that the AO erosion is confined to the epoxy, with the mica particles able to flake off. The mica flakes are also seen to be oriented parallel to the surface. This confirms the proposed literature model that attributed the increased resistance to AO by mica to be due to preferred orientation of the mica particles, creating an inorganic barrier to attack. The surface morphology of the unashed and ashed 37.25/37.25 composition is shown in Figure 4. The fiber pattern appears different because the surfaces are from two different samples. Nonetheless, it is seen that the erosion has exposed both the mica and glass fibers. Furthermore, there is erosion below the glass fibers, indicating that the glass fibers do not offer increased resistance and are free of the surface. This confirms the increase in mass loss and the AE data of Figures 14 (B) and 16 (B) in which the large number of events are attributed to friction and breakage of the unbonded fibers. Figure 5 shows the unashed and ashed surface morphologies of the all-glass-fiber composites. The erosion is observed to penetrate at least three fiber diameters, leaving many loose fibers on the surface. This supports the proposed source of the increased AE in this composition, which is the same as the 37.25/37.25 composition. Also, it is apparent that the glass fibers do not hinder the erosion of the epoxy and thus this composite erodes the most.

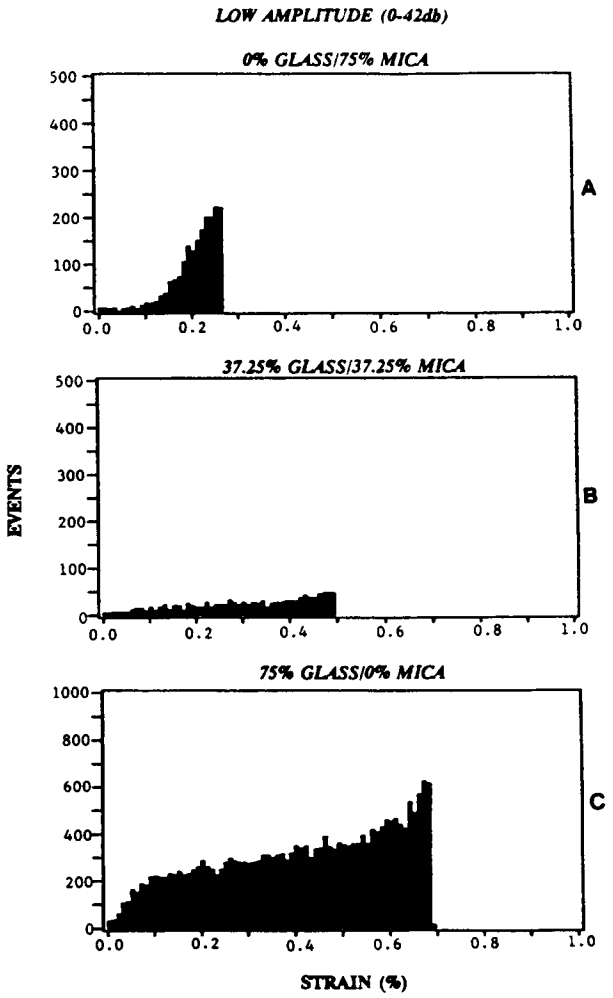

Figure 14. Amplitude analysis of the exposed to AO composites showing the low-amplitude (0–42 db) events vs. strain.

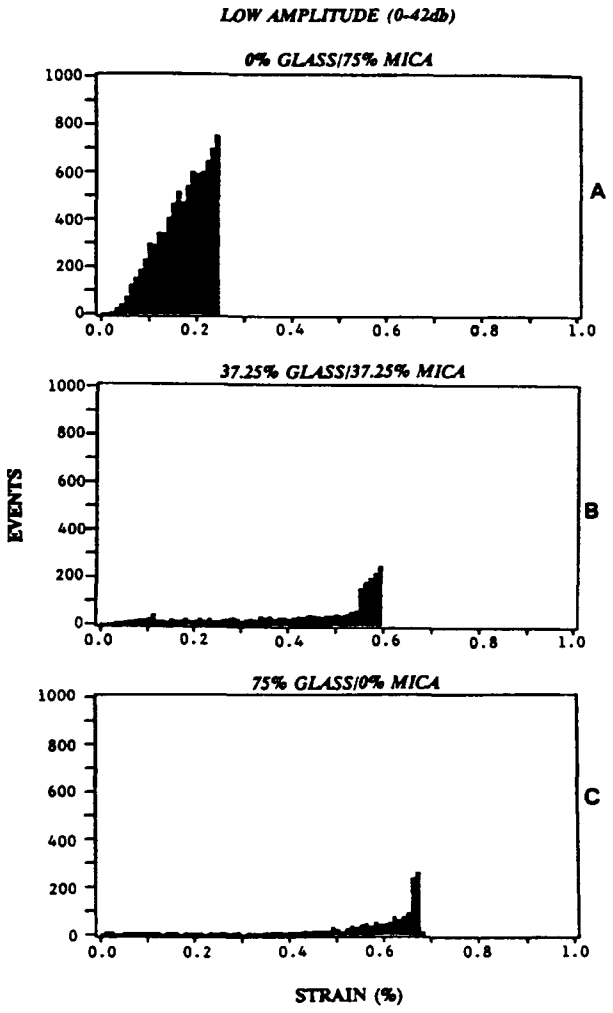

Figure 15. Amplitude analysis of the unexposed composites showing the low-amplitude (0–42 db) events vs. strain.

EDAX of Composite Surfaces

The EDAX of the surfaces are shown in Figures 6–8. Inspection of these reveals that the carbon peak is the only peak of interest that changes; that is, the carbon peak disappears upon ashing, indicating that the epoxy is being oxidized and volatilized in agreement with the literature.[2] The palladium peak is also observed to change in height. This is due to differences in the thickness of the coatings.

Fracture Surfaces of Composites

The fracture surfaces of the ashed composites, shown in Figures 9–11, exhibit no differences from the unashed composites. This would be expected since the ashing is a surface phenomena only and the fracture surfaces represent the bulk behavior. One difference, however, can be seen in the all-glass-fiber composite shown in Figure 11. The low-magnification micrograph [Fig. 11(a)] shows the loose fibers on the surface.

Flexural Properties

Table II shows the effect of AO on the flexural properties of the composites. Because the mechanical property measurements are based on two different sample sets, which had different thicknesses, the flexural properties are given in their most basic form and are corrected for these differences. Furthermore, the exposure to AO created a surface layer that was easily removed. This layer was assumed to have no mechanical integrity, so was accounted for in the property calculations by removing this layer and using the reduced thickness. Comparison of the un-

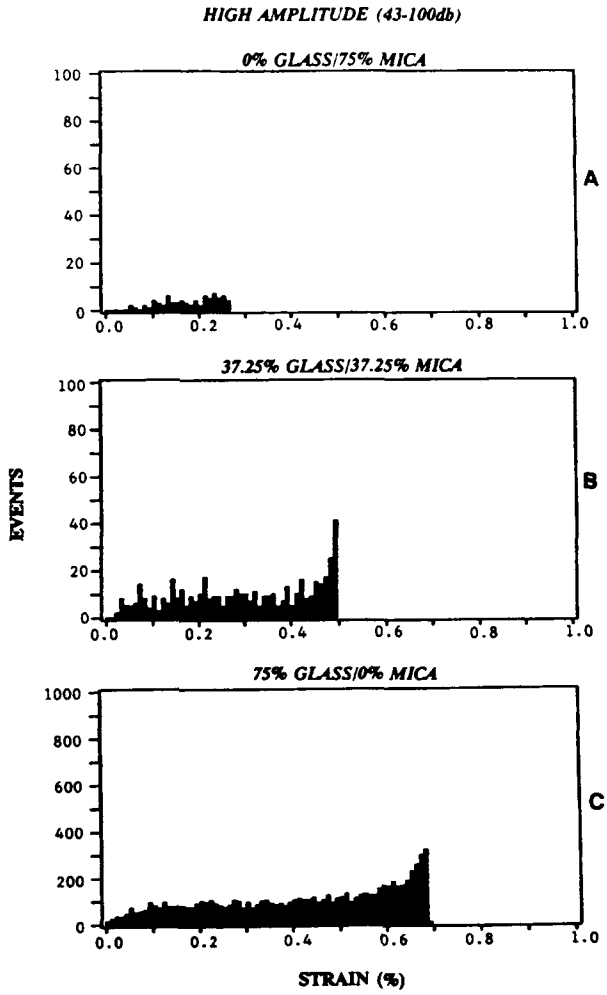

Figure 16. Amplitude analysis of the exposed to AO composites showing the high-amplitude (43–100 db) events vs. strain.

ashed and ashed (scraped) columns reveals an insignificant drop in the initial slope, maximum load, and maximum deflection due to standard deviations that are approximately ± 10%. A change in the mechanical properties is not expected since the SEM studies have shown that AO erosion is confined to the surface. This has been observed by other researchers.[2,8,16]

Acoustic Emission during Flexural Deformation

Damage Analysis by Amplitude Segregation

Since the ashed 0/75 composite exhibited a similar amplitude distribution, shown in Figure 12, as the unashed composite shown in Figure 13, the amplitude distribution was divided into low (0–42 db) and high (43–100 db) amplitude regions in the same manner as were the unashed composites. Figure 14(A) shows the damage accumulation of the low-amplitude events. The all-mica composite still exhibits a linear increase in events, like the unashed composite does, Figure 15(A), but has an initial region with very few events, whereas the unashed composite's increase started almost immediately. The cause of this is not obvious. However, it must be related to the erosion of the surface layer, which has been shown to be epoxy. Figure 14(B) shows the damage accumulation of the low-amplitude events of the ashed 37.25/37.25 composition. The events increase throughout the deformation with a slight increase just prior to failure. This is in contrast to the unashed composition, shown in Figure 15(B), where there are few events until just prior to failure. As the SEM surface morphology and fracture surfaces have shown, there are a multitude of loose fibers on the eroded surface. The rubbing together of these fibers can create "noise" that can account for the large number of events observed throughout the deformation process. Figure 14(C) shows the damage accumulation of the low-amplitude events of the ashed 75/0 composition. Not only do the events increase throughout the deformation process with a slight increase just prior to failure, but there are a very large number of events. This is in stark contrast to the unashed composition, shown in Figure 15(C), where very few events occur until just prior to failure. The explanation given is the same as for the 37.25/37.25 composition. The much larger number of events are detected because the surface is eroded to a deeper depth, exposing many more fibers, which create more "noise."

The high-amplitude events (43–100 db) are shown in Figure 16. The all-mica composite, shown

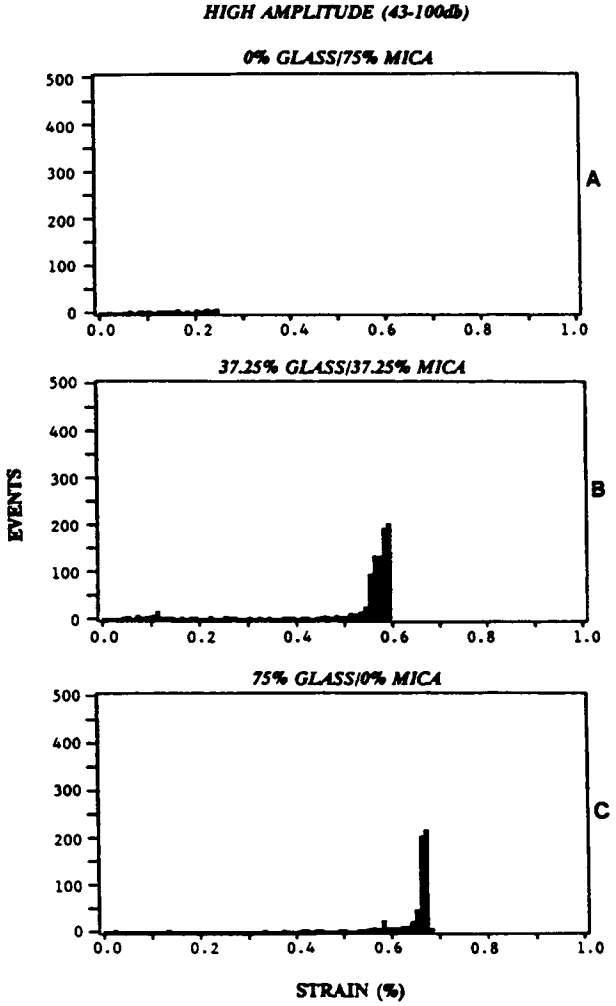

Figure 17. Amplitude analysis of the unexposed composites showing the high-amplitude events (43–100 db) vs. strain.

in Figure 16(A), has an insignificant amount of events. Figure 16(B) shows the high-amplitude events for the ashed 37.25/37.25 composite. High-amplitude events occur almost immediately and continue throughout the deformation process with an increase just prior to failure. Since it was previously determined that the high-amplitude events are caused by fiber breakage and fiber pullout at high strains only, Figure 17(B), the occurrence of this amplitude at low strains is not expected. However, the surface morphology holds the key as it was already reported that a multitude of loose glass fibers are present on the eroded surface. Not only can these fibers create noise by rubbing together, they are also very brittle and can easily break at low strains during flexure. This has been observed by Rutledge et al.[8] The all-glass-fiber composite exhibits similar behavior as does the 37.25/37.25 composition but has

a much higher number of events. This is explained in the same manner with the high number of events due to the higher content of glass fibers plus the deeper erosion, which frees more fibers.

The hypothesis that the loose fibers are causing the additional low- and high-amplitude events was confirmed by exposing the composites to AO for 7 days, removing the loose fibers, and retesting the composites under the same conditions as the exposed (without fiber removal) compositions. The large number of low-amplitude events and the occurrence of high-amplitude events at low strains was not observed, indicating that the loose fibers were the cause of these events.

Prefailure Analysis as a Function of Composition

Figure 12 shows the AE compositional analysis for the ashed composites. The 0/75 composite [Fig. 12(A)] has a similar amplitude distribution as does the unashed composite, shown in Figure 13(A), indicating the damage mechanism is unchanged. As soon as the glass fiber is added to the composition, more than one peak is present as shown in Figure 12 (B and C), which is similar to the unashed composites. The actual amplitude histograms appear slightly different, however, so no quantitative conclusions can be drawn from this. It is therefore concluded that the damage mechanisms have not changed. This confirms the fact that the mechanical properties did not significantly change, as a change in damage mechanisms would be expected to change the mechanical properties.

CONCLUSIONS

1. As the mica content increases, the resistance to atomic oxygen increases (as measured by the mass loss, ashing rate, and reaction efficiency) over one order of magnitude from the all-glass-fiber composite to the all-mica composite. This is caused by mica preferentially orienting parallel to the surface, creating an inorganic barrier to attack.
2. AO does not significantly affect the flexural properties or prefailure damage mechanisms because the erosion is confined to the epoxy surface only and does not affect the bulk. However, the erosion of the surface creates more AE events at low strains because of breakage of the loose fibers and noise generated by the loose fibers rubbing together.

Financial support was provided by the NASA-CCDS Materials for Space Structures.

REFERENCES

1. R. A. Cull, Paper presented at a Meeting of the Rubber Division, ACS, Dallas, TX, April 19–22, 1988, Paper #55.
2. W. S. Slemp, B. Santos-Mason, G. F. Sykes, Jr., and W. G. Witte, Jr., *Effects of STS-8 Atomic Oxygen Exposure on Composites, Polymeric Films, and Coatings,* Atomic Oxygen Effects Measurements for Shuttle Missions STS-8 and 41-G, Vol. I, Section 5, NASA Technical Memorandum 100459, 1988, pp. 1–15.
3. C. K. Purvis, *Overview of Environmental Factors,* NASA/SDIO Space Environmental Effects on Materials Workshop, NASA Conference Publication 3035, Part I, Section 1, Session 1, 1988, pp. 5–24.
4. D. R. Tenney, *Structural Materials for Space Applications,* NASA Conference Publication 3035, Part I, Section 1, Session 1, 1988, pp. 25–52.
5. D. E. Bowles and D. R. Tenney, *SAMPE J.* **May/June,** 49–57 (1987).
6. J. T. Visentine, *Environmental Definition of the Earth's Neutral Atmosphere,* NASA Conference Publication 3035, Part I, Section 1, Session 3, 1988, pp. 179–195.
7. S. Rutledge, B. Banks, F. DiFilippo, J. Brady, T. Dever, and D. Hotes, *An Evaluation of Candidate Oxidation Resistant Materials for Space Applications in LEO,* NASA Technical Memorandum 100122, 1986.
8. S. K. Rutledge, P. E. Paulsen, J. A. Brady, and M. L. Ciancone, *Oxidation and Protection of Fiberglass-Epoxy Composite Masts for Photovoltiac Arrays in the Low Earth Orbital Environment,* NASA Technical Memorandum 100839, 1988.
9. J. C. Gregory, in *Proceedings of the NASA Workshop on Atomic Oxygen Effects,* Jet Propulsion Laboratory, Pasadena, CA, November 10–12, 1986.
10. J. C. Gregory and P. N. Peters, *Polym. Prepr.* **28**(2), 459–460 (1987).
11. P. N. Peters, *Polym. Prepr.* **28**(2), 459–460 (1987).
12. L. J. Leger and J. T. Visentine, *J. Spacecraft,* **23**(5): 505–511 (1986).
13. D. G. Zimcik and C. R. Maag, *Results of Apparent Atomic Oxygen Reactions with Spacecraft Materials,* Atomic Oxygen Effects Measurements for Shuttle Missions STS-8 and 41-G, Vol. I, Section 10, NASA Technical Memorandum 100459, 1988, pp. 1–10.
14. J. T. Visentine, *Atomic Oxygen Effects Experiments: Current Status and Future Directions,* Atomic Oxygen Effects Measurements for Shuttle Missions STS-8 and 41-G, Vol. III, NASA Technical Memorandum 100459, 1988, pp. 1–19.
15. R. L. Kiefer and R. A. Orwoll, *Space Environmental Effects on Polymeric Materials,* Final Technical Report, NASA Research Grant NAG-1-68, 1988.
16. R. H. Hansen, J. V. Pascale, T. DeBenedictis, and P. M. Rentzepis, *J. Polym. Sci. A,* **3,** 2205–2214 (1965).

Received July 12, 1990
Accepted August 15, 1990